Ginzburg-Landau-Type Multiphase Field Model for Competing fcc and bcc Nucleation

G. I. Tóth, J. R. Morris, and L. Gránásy

Ginzburg-Landau type multi-phase-field model for competing fcc and bcc nucleation

G. I. Tóth,[1] J. R. Morris,[2] and L. Gránásy[1,3]

[1]*Research Institute for Solid State Physics and Optics, P. O. Box 49, H-1525 Budapest, Hungary*
[2]*Oak Ridge National Laboratory, Oak Ridge, TN 37830, USA*
[3]*BCAST, Brunel University, Uxbridge, Middlesex, UB8 3PH, UK*

We address crystal nucleation and fcc-bcc phase selection in alloys using a multi-phase-field model that relies on Ginzburg-Landau free energies of the liquid-fcc (face centered cubic), liquid-bcc (body centered cubic), and fcc-bcc sub-systems, and determine the properties of the nuclei as a function of composition, temperature and structure. With a realistic choice for the free energy of the fcc-bcc interface, the model predicts well the fcc-bcc phase-selection boundary in the Fe-Ni system.

Freezing of undercooled liquids often starts with the nucleation/formation of metastable (MS) crystalline phases. In agreement with Ostwald's step rule, atomistic simulations imply that the first crystal structure to form is the one, whose free energy is the closest to the free energy of the liquid [1]. In alloys this represents a multi-phase multi-component solidification problem. To date, the most efficient method used for addressing such problems is the multi-phase-field theory (MPFT) [2]. It is, however, only as accurate as the free energy functional it relies on. Early versions [2] of the MPFT predicted that the third phase inevitably appears at the interface between two bulk phases, a behavior originating from the specific free energy surface assumed. A recent version of MPFT eliminated the third phase entirely at the interface [3]. This is not always in agreement with real systems: Atomistic simulations for the Lennard-Jones (LJ) system show that although the stable phase is fcc, small nuclei have a bcc structure, and even the larger fcc crystallites have a bcc-like layer at the solid-liquid interface [1, 4], results also born out by the classical density functional theory (CDFT) [5]. These findings accord with the theoretical prediction of Alexander and McTague that in simple liquids the formation of bcc structure is preferred [6]. Further simulations for the LJ system imply that varying the pressure at fixed temperature, the bcc/fcc phase ratio can be tuned in small clusters [7]. Since preference for MS phase nucleation is quite general, it is desirable to work out microscopic models that can handle the structural aspects of phase selection during nucleation.

In this Letter, we present such a microscopic model for competing fcc and bcc structures. The MPFT is supplemented with a free energy that is based on the GL expansion of the two-phase free energies [8–10], and considers thus the structural aspects of multiphase solidification. Our approach is unique in that it combines crystal structure with thermodynamic and interfacial data of real systems. In this respect our MPFT is more flexible than recent CDFT approaches [11], which, in turn, pro-

vide a more detailed description of the solid-solid interface. Herein, we apply the GL-free-energy based MPFT to predict phase-selection in the Fe-Ni system.

The standard MPFT form of the grand free energy of a binary system relative to the initial liquid is:

$$\Delta\Omega = \int d\mathbf{r} \left\{ \sum_{i<j} \frac{\epsilon_{ij}^2}{2} \left(\phi_i \nabla \phi_j - \phi_j \nabla \phi_i \right)^2 + \Delta\omega(\phi_i, c) \right\}.$$

(1)

The differential operator on the right hand side has the required symmetries [2]. In this expression $\Delta\omega$ is the relative grand potential density and c the concentration. The sum runs over different (ϕ_i, ϕ_j) pairs of the structural order parameters, while $\sum_j \phi_j(\mathbf{r}) = 1$. When addressing fcc-bcc competition, without loss of generality, we may chose ϕ_1, ϕ_2, and $\phi_3 = 1 - (\phi_1 + \phi_2)$ for the fcc, bcc, and liquid phases, respectively. These order parameters can be combined to yield formal analogues of the solid-liquid order parameter m that describes crystalline freezing, and the solid-solid order parameter χ that monitors the fcc-bcc transition (Bain's distortion) of the crystal lattice used in an advanced CDFT of fcc-bcc transition [5]: $\phi \Leftrightarrow ||m|| \in [0, 1]$ and $\psi \Leftrightarrow ||\chi|| \in [0, 1]$, where $\phi = \phi_1 + \phi_2$ and $\psi = \phi_2/\phi$. The methodology of the MPFT anchors the free energy surface to the free energies of the bulk phases. Specifically, the local grand potential density of the multi-phase system is related to the contributions $\Delta\omega_{ij}$ of the two-phase systems as follows:

$$\Delta\omega(\phi, \psi, c) = [1 - p_{12}(\psi)]\Delta\omega_{13}(\phi, c) + \\ + p_{12}(\psi)\Delta\omega_{23}(\phi, c) + a_{12}(c)P(\phi, \psi)g_{12}(\psi),$$

(2)

where the interpolation functions p_{ij} vary monotonously between 0 and 1 so that $p_{ij}(0) = 0$ and $p_{ij}(1) = 1$, whereas $P(\phi, \psi) = [1 - p_{12}(\psi)]p_{13}(\phi) + p_{12}(\psi)p_{23}(\phi)$, which reflects that the solid-solid order parameter is irrelevant in the liquid state. The first two terms of Eq. (2) interpolate between the fcc-liquid and bcc-liquid free energies, while the third term adds a free energy barrier
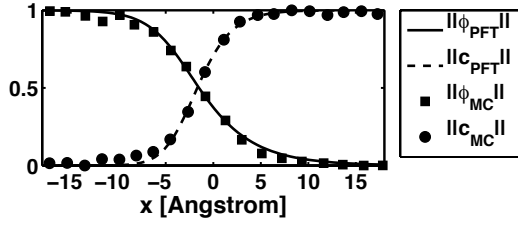
FIG. 1: Interfacial order parameter (solid) and concentration profiles (dashed) as predicted by the GL approach for the fcc-liquid interface in the Cu-Ni system. For comparison, the normalized density peaks (squares) and concentration profile (circles) from atomistic simulations [15] are also shown.

in between the two solid phases that disappears in the liquid. The two-phase contributions can be expressed as

$$\Delta\omega_{i3}(\phi,c) = a_{i3}(c)g_{i3}(\phi) +$$
$$+ p_{i3}(\phi)\Delta\omega_i(c) + [1 - p_{i3}(\phi)]\Delta\omega_3(c),$$

for $i = 1$ or 2, which have the shape of a skewed double-well. Here g_{ij} are double-well functions, for which $g_{ij}(0) = g_{ij}(1) = 0$, with a maximum in between, while the functions $\Delta\omega_i$ represent the grand potential densities of the ith phase relative to the initial liquid state.

With these definitions, Eq. (2) recovers the relative free energies of the bulk phases. However, the results for the non-bulk states depend on the specific choice of these functions. In the usual application of the MPFT, they are chosen intuitively. In contrast, here we use forms deduced from the GL expansion of the two-phase free energies [8–10], which forms contain the structural information:

bcc-liquid: $g_{13} = \phi^2(1-\phi)^2$ and $p_{13} = \phi^3(4-3\phi)$,
fcc-liquid: $g_{23} = \phi^2(1-\phi^2)^2$ and $p_{23} = \phi^4(3-2\phi^2)$,
bcc-fcc: $g_{12} = \psi^2(1-\psi)^2$ and $p_{12} = \psi^3(4-3\psi)$.

The composition dependent model coefficients are interpolated as $\epsilon_{ij}^2(c) = (1-c)\epsilon_{ij,A}^2 + c\epsilon_{ij,B}^2$ and $a_{ij}(c) = (1-c)a_{ij,A} + ca_{ij,B}$, where the constants $\epsilon_{ij,Y}^2$ and $a_{ij,Y}$ can be expressed in terms of the free energy and thickness of the equilibrium interface between phases i and j for pure component Y. Unlike the CDFT, where the time-averaged particle density is the order parameter, in our model the solid-liquid transitions are monitored by the reduced Fourier amplitude of the dominant density waves (a single-mode approach), whereas the fcc-bcc transition by an order parameter related to Bain's distortion. The free energy of the interfaces emerge from bulk and gradient contributions associated with a continuous change of these order parameters across the interface.

Since the nucleus represents an extremum of the grand potential, its properties can be found by solving the Euler-Lagrange (EL) equations [5, 9, 12]: $\delta\Delta\Omega/\delta\phi_i = \lambda(\mathbf{r})$ and $\delta\Delta\Omega/\delta c = 0$, where $\delta\Delta\Omega/\delta\eta$ is the first functional derivative of the grand potential difference with
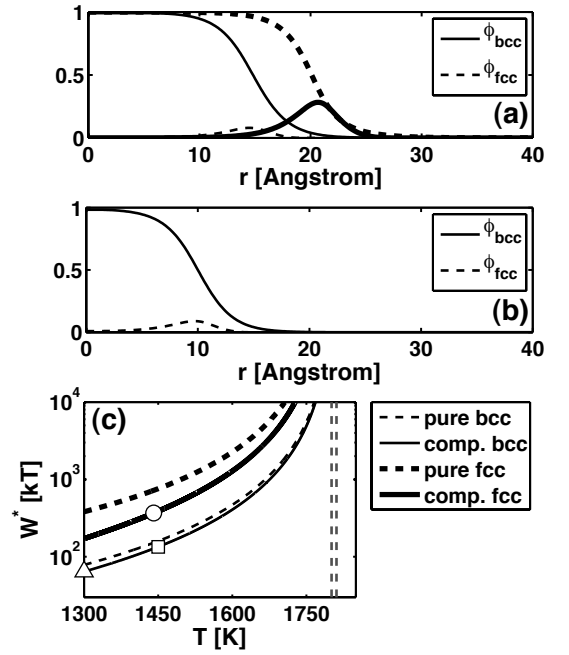

FIG. 2: Crystal nuclei in Fe: (a) composite-bcc nucleus at 1449 K [thin lines, square in panel(c)], and composite-fcc nucleus at 1441 K [heavy lines, circle in panel (c)]; (b) composite-bcc nucleus at 1300 K [triangle in panel(c)]. (c) Nucleation barrier vs. temperature.
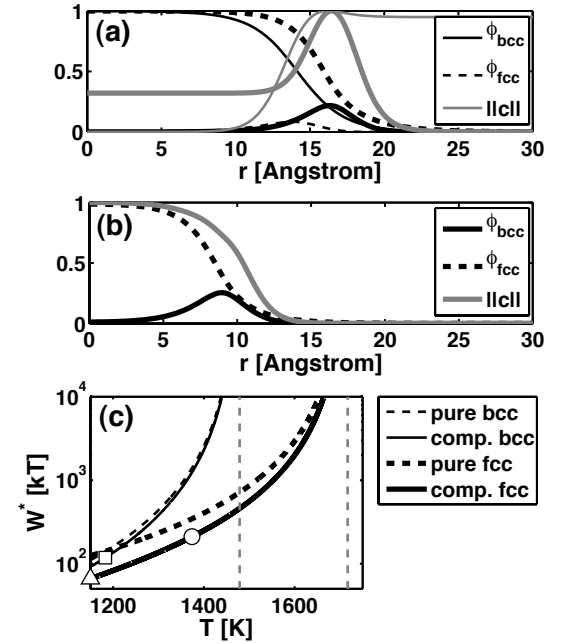

FIG. 3: Crystal nuclei in Fe$_{50}$Ni$_{50}$: Notations are as for Fig. 2. The respective temperatures are $T = 1373.5$ K and 1183 K for panel (a) and 1150 K for panel (b). Note that $||c|| \in [0, 1]$.
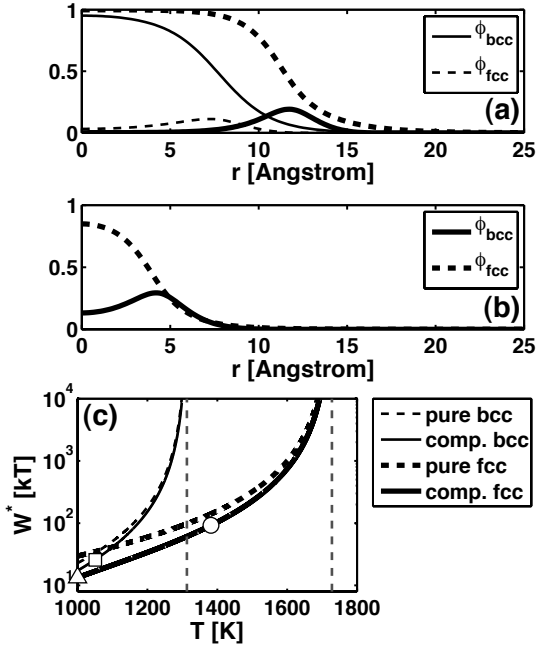
FIG. 4: Crystal nuclei in Ni: Notations are as for Fig. 2. The respective temperatures are $T = 1382.5$ K and 1050 K for panel (a) and 1000 K for panel (b).
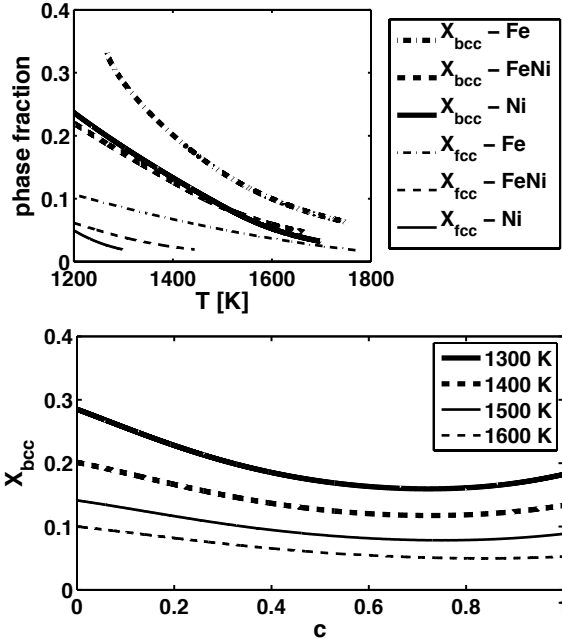

FIG. 5: Volume fraction of the third phase ("surface phase") in composite nuclei: (a) Temperature dependence of bcc fraction in composite-fcc nuclei (heavy lines), and of fcc fraction in composite-bcc nuclei (thin lines). (b) bcc fraction vs. Ni concentration at different temperatures.

respect to the field η, while the Lagrange multiplier $\lambda(\mathbf{r})$ ensures the local constraint $\sum_j \phi_j(\mathbf{r}) = 1$ [13]. The respective boundary conditions are as follows: unperturbed liquid properties in the far field and zero field gradients at the center. We assume isotropic interfacial properties, a fair approximation for metallic systems. This boundary value problem has been solved numerically by the relaxation method. The excess free energy of the nuclei has been obtained by inserting the solution into Eq. (1).

The two-phase limits of the present model have been tested previously: The GL technique proved successful in describing (i) the nucleation barrier for fcc structure [9], (ii) the properties of the bcc-liquid interfaces [8, 14], and (iii) the transition between the bcc and fcc phases [10]. The chemical part of our model has been tested against atomistic simulations for the Cu-Ni system: The parameter free GL predictions for the order-parameter and nanoscale concentration profiles are in a remarkable agreement with the Monte Carlo results [15] (Fig. 1).

Owing to the lack of known equilibrium coexistence conditions between the bulk fcc and bcc phases, the well-known LJ and hard-sphere systems are not suitable for a full testing of our model. Thus, we have chosen the Fe-Ni system, where from combined experiments and atomistic simulations a nearly complete input set is available [16]. The least accurate input is the orientation average of the free energy of the fcc-bcc interface. For Fe, estimates of $\gamma_{fcc-bcc}$ for different orientations range between 179 mJ/m^2 [17] and about twice the solid-liquid interfacial energy ($\sim$672 mJ/m^2 [16]), yielding $\sim$425 mJ/m^2 for the average of the upper and lower limits, which we take as an estimate of the orientation average. Thus the energy contribution of the defects at the fcc-bcc interface is incorporated implicitly in a coarse-grained manner.

First, we present our results for crystal nuclei in Fe, Fe$_{50}$Ni$_{50}$, and Ni (see Figs. 2–4). In panels (a) and (b), the radial phase-field and concentration profiles are displayed. In all cases we observe at least a small amount of third phase ("surface phase") at the solid-liquid interface. However, the fcc surface layer on bcc nuclei is far less pronounced than the bcc layer on fcc nuclei [Fig. 5(a)]. With increasing undercooling, the volume fraction (X) of the third phase increases [Fig. 5(a)], which is reflected in the non-monotonic composition dependence of X [Fig. 5(b)], following from the shape of the respective liquidus line in the phase diagram. In Fe, nuclei with a bcc core (composite-bcc type) are significantly preferred to fcc core nuclei, whereas in Ni, at temperatures accessible for experiments, composite-fcc nuclei with a bcc surface layer dominate [see Figs. 2(c) and 4(c)]. The nuclei observed at the 1:1 composition behave similarly to those for Ni [Fig. 3(c)], however, with some amount of surface precipitate of Ni at 20% relative undercooling [Fig. 3(a)]. At extremely large undercoolings, composite-bcc nuclei are preferred for all compositions. At all undercoolings we studied, composite nuclei are thermodynam-
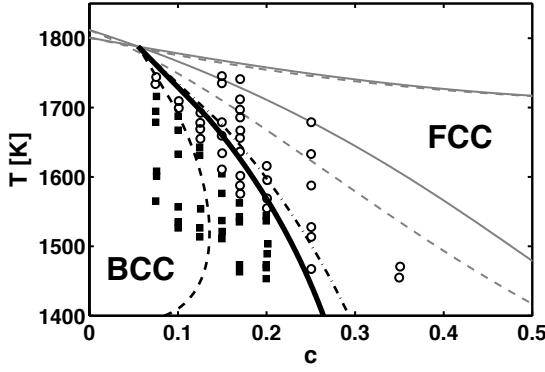
FIG. 6: Phase-selection in the Fe-Ni alloy system. The grey solid and dashed lines correspond to the liquidus and solidus curves. The symbols indicate the structure nucleated in the experiment: squares - bcc; circles - fcc [18]. The fcc-bcc phase-selection boundary predicted for heterogeneous nucleation at three values of $\gamma_{fcc-bcc}$ are shown: 672 (black dash-dot), 425 (black solid), and 179 mJ/m^2 (black dashed).

ically preferable to the respective single-phase nuclei.

Next, we use the present MPFT approach to predict the phase-selection map for Fe-Ni alloys and compare it to experiments [18]. Since in metallic systems homogeneous nucleation has probably never been realized, we assume heterogeneous nucleation. In the spirit of the highly successful free growth limited model of heterogeneous nucleation by Greer et al. [19], the phase-selection boundary for heterogeneous nucleation is determined by the condition of equal critical radii for the fcc and bcc type nuclei. The fcc-bcc phase-selection boundary predicted with $\gamma_{fcc-bcc} = 425$ mJ/m^2 is in a fair agreement with the experiments (Fig. 6). For comparison, results for the upper and lower limits are also shown, which envelope the experimental fcc-bcc phase-selection boundary.

Summarizing, we have presented a microscopic multiphase-field theory of competing fcc and bcc nucleation that is anchored to measurable physical properties. Our study indicates that composite nuclei are preferable to single-phase nuclei. With a reasonable choice of model parameters, the GL-free-energy based MPFT predicts the phase-selection map fairly well for Fe-Ni alloys.

[1] P. R. ten Wolde and D. Frenkel, Phys. Chem. Chem. Phys. **1**, 2191 (1999).
[2] I. Steinbach et al., Physica D **94**, 135 (1996).
[3] R. Folch and M. Plapp, Phys. Rev. E **72**, 011602 (2005).
[4] P. R. ten Wolde et al., Phys. Rev. Lett. **75**, 2714 (1995).
[5] Y. C. Shen and D. W. Oxtoby, Phys. Rev. Lett. **77**, 3585 (1996).
[6] S. Alexander and J. McTague, Phys Rev. Lett. **41**, 702 (1978); W. Klein, Phys. Rev. E. **64**, 056110 (2001).
[7] C. Desgranges and J. Delhommelle, Phys. Rev. Lett. **98**, 235502 (2007); J. Am. Chem. Soc. **128**, 10368 (2006).
[8] W. H. Shih et al., Phys. Rev. A **35**, 2611 (1987).
[9] L. Gránásy and T. Pusztai, J. Chem. Phys. **117**, 10121 (2002); G. I. Tóth and L. Gránásy, J. Phys. Chem. B **113**, 5141 (2009).
[10] V. P. Dimitriev et al., Phys. Rev. B **44**, 7248 (1991).
[11] K. R. Elder et al., Phys. Rev. Lett. **88**, 245701 (2002); A. Jaatinen et al., Phys. Rev. E **80**, 031602 (2009).
[12] L. Gránásy et al., Phys. Rev. Lett. **88**, 206105 (2002); **98**, 035703 (2007).
[13] The EL equations are: $\mathbf{M}(\Phi, c)\Delta\Phi^T = \mathbf{b}(\Phi, c, \nabla\Phi, \nabla c)$ and $2\partial_c\Delta\omega + \sum_{i<j} \partial_c\epsilon_{ij}^2(c)(\phi_i\nabla\phi_j - \phi_j\nabla\phi_i)^2 = 0$. Here $\Phi = (\phi_1, \phi_2)$, $\Delta\Phi = (\Delta\phi_1, \Delta\phi_2)$, superscript T denotes transposition, $b_i = E_i - E_3$, whereas $E_i = \partial_{\phi_i}\Delta\omega + \sum_{i\neq j}\left[\partial_c\epsilon_{ij}(c)^2\nabla c + 2\epsilon_{ij}(c)^2\nabla\phi_j\right](\phi_i\nabla\phi_j - \phi_j\nabla\phi_i)$, and the elements of the 2×2 matrix $\mathbf{M}$ are: $M_{11} = \epsilon_{13}^2(1 - \phi_2)^2 + (\epsilon_{12}^2 + \epsilon_{23}^2)\phi_2^2$; $M_{22} = \epsilon_{23}^2(1 - \phi_1)^2 + (\epsilon_{12}^2 + \epsilon_{13}^2)\phi_1^2$; and $M_{12} = M_{21} = \epsilon_{13}^2\phi_1(1-\phi_2) + \epsilon_{23}^2\phi_2(1-\phi_1) - \epsilon_{12}^2\phi_1\phi_2$.
[14] K.-A. Wu et al., Phys. Rev. B **73**, 094101 (2006).
[15] H. Ramalingam et al., Interf. Sci. **10**, 149 (2002).
[16] Free energy of bulk phases: Y. Y. Chuang, K. C. Shieh, and Y. A. Chang, Metall. Trans. A **17**, 1373 (1986). Interface thickness: 1 nm for all interfaces, [$\sim$ 3.5 atomic distances: B. B. Laird and A. D. J. Haymet, Chem. Rev. **47**, 2491 (1993)]. Solid-liquid interface energy of Fe and Ni at the melting point (T^f): L. Gránásy and M. Tegze, Mater. Sci. Forum **77**, 243 (1991). Interface energy of MS phases: The ratio $\alpha_{fcc}/\alpha_{bcc} \approx 1.72$ deduced for Turnbull's coefficients from atomistic simulations for Fe [D. Y. Sun, M. Asta, and J. J. Hoyt, Phys. Rev. B **69**, 174103 (2004)] was used to estimate it: $\gamma_{MS}/\gamma_S \approx (\alpha_{MS}T_{MS}^f)/(\alpha_S T_S^f)$. We utilized Richard's rule and neglected the density difference of the crystalline phases. Here $\alpha = \gamma L^{-1}\rho^{-2/3}$, γ the interface energy, L the heat of fusion, and ρ the singlet density. Subscript S denotes the stable phase.
[17] J. K. Chen et al., Acta Mater. **45**, 4415 (1997).
[18] A. Zambon et al., Acta Mater. **46**, 4657 (1998).
[19] A. L. Greer et al., Acta Mater. **48**, 2823 (2000).